Classification
Physics Abstracts
06.50 — 07.80 — 78.70

Determination of inner-shell cross-sections for EELS-quantification

Ferdinand Hofer

Forschungsinstitut für Elektronenmikroskopie und Feinstrukturforschung, Graz University of Technology, A-8010 Graz, Austria

(Received October 02, 1990; accepted March 26, 1991)

Abstract. — Quantitative microanalysis using the EELS technique requires the knowledge of partial scattering cross-sections to relate the measured intensities to the concentrations in the compounds. Partial scattering cross-sections can be determined either theoretically or empirically by means of standards. Cross-sections for K, L_{23} and M_{45} ionization edges can be calculated by the hydrogenic model and by the Hartree-Slater-model and with these models elements ranging from Li to W can be quantified. Alternatively, the ratio of two cross-sections (k-factor) can be used for quantification. These k-factors can be determined by measuring the appropriate ionization edges using a thin film standard, which has been done for K, L_{23}, M_{45} and N_{45}-edges. Scattering cross-sections which have been determined by these methods are compared and their impact on the reliability and accuracy of EELS-quantification is critically discussed.

1. Introduction.

EELS is an important technique for microanalysis in the analytical electron microscope. Until recently it has been used mainly for the analysis of light elements. However, ratios of light to heavier elements such as second row transition elements and rare earth elements have become of interest in ceramic materials (e.g. high T_C-superconductors).

Elemental analysis by EELS is enabled by the inner-shell edges, the position and intensity of which can be used to identify and quantify atomic species within the sample. The quantification of the EELS-spectra requires the knowledge of partial scattering cross-sections, i.e. differential cross-section integrated over angle and energy. These cross-sections can be determined either theoretically, or experimentally by using standards, and are one possible source of error in EELS-quantification.

Although considerable attention has been paid to the development of methods for quantification of EELS-spectra some problems remain in fully quantifying such data, such as:

1) specimen thickness limitations,
2) reliability of background extrapolations and
3) uncertainties in case of partial scattering cross-sections.

The first two points and the general procedures for EELS-quantification have been extensively discussed by Egerton [1]. The third point is the topic of this contribution, because an accurate

knowledge of scattering cross-sections is not only useful for their practical application to spectral quantification procedures but provide a necessary guide to the development and refinement of theoretical models for electron-solid interactions.

It is our aim to review and compare diverse methods for the determination of scattering cross-sections, to enquire into the reliability of these methods and the accuracy obtainable.

2. Procedure of quantification.

In practical EELS-microanalysis, mainly relative concentrations are used and they can be determined according to the following equation [2],

$$\frac{N_A}{N_B} = \frac{I_A(\beta, \Delta) \cdot \sigma_B(\beta, \Delta)}{I_B(\beta, \Delta) \cdot \sigma_A(\beta, \Delta)}$$

where

N_i is the number of atoms per unit area

$I_i(\beta, \Delta)$ is the core loss intensity integrated up to an energy region of width Δ starting at the edge onset

$\sigma_i(\beta, \Delta)$ is the partial scattering cross-section integrated over a collection angle β and an energy region Δ.

Although this equation is straightforward, several problems and limitations must be taken into account when quantification is performed [3,4].

The experimental requirements for quantitative EELS and also for the experimental determination of partial cross-sections are summarized in the following:

a) Specimen thickness: Specimens should be as thin as possible; at least thinner than the half of the mean free path of inelastic scattering, otherwise the spectrum must be deconvoluted [5,6].

b) Beam convergence: If the incident convergence angle is comparable to the value of the collection angle β, a convergence correction has to be applied [7].

c) Orientation effects: Crystalline samples should be orientated in a way so that no strongly diffracted beams are excited [8].

d) Lens aberration effects: Chromatic aberration can degrade the intensities at high energy-losses and large collection angles. This effect is especially significant when the spectra are recorded in TEM-diffraction coupling (TEM-image mode) [4,7,9].

3. Determination of partial scattering cross-sections.

3.1 CALCULATION OF CROSS-SECTIONS. — In practical microanalysis standardless quantification is mainly used, because it can be performed rapidly using calculated cross-sections. Since the inner-shell cross-section is primarily atomic in nature, the theoretical approaches are based on atomic models:

3.1.1 *Hydrogenic model.* — The most widely used method of calculating partial cross-sections is the hydrogenic model which has been introduced by Egerton [10]. The cross-sections are calculated assuming an atomic model, based on hydrogenic wavefunctions which are scaled to take account of the nuclear charge and incorporate a single atomic-number dependent constant to account for screening.

The hydrogenic model predicts saw tooth profiles and is therefore directly applicable to the quantification of the K ionisations, the edges of which exhibit almost saw tooth profiles. A short

computer program written by Egerton (SIGMAK) [10,11] allows quantification of the elements ranging from Li to Si.

A hydrogenic model was also developed for L-shells, but here the simple treatment of screening proves inadequate and empirical factors have been inserted to match experimentally determined edge shapes. The computer program of Egerton [12] has been improved several times and the latest version denoted SIGMAL2 [3] also takes account of the white lines at the edge-onset. The SIGMAL2 program allows quantification of the elements ranging from Al-Zn.

However, for quantification of heavier elements ($Z > 30$) higher order ionizations such as M or N edges must be used, and a hydrogenic model for these edges would require substantial correction near the ionization threshold. Recently Luo and Zeitler [13] corrected the hydrogenic results for M-shells by means of experimental photoabsorption data.

3.1.2 *Hartree-Slater-model.* — This method can be applied to all inner shells and to heavy elements as well. However, the calculations are relatively extensive [14,15]. Elements ranging from Li to W can be quantified. The theoretical cross-sections used here are derived from a Hartree-Slater central field model. This model assumes the elements are in atomic form and can be treated on the basis of a single electron inner-shell wave function undergoing a transition to the continuum. No solid state or excitonic effects or transitions to unoccupied bound states are taken into account.

3.1.3 *Other methods.* — A further method has been described by Skiff *et al.* [16] and recent calculations of H. Kohl and coworkers yielded results comparable to the Hartree-Slater model [17].

3.2 Experimental determination of cross-sections.

3.2.1 *Standard-method.* — This method has general applicability and can be used for many elements ranging from Li to U [18]. A difficulty associated with measuring cross-sections is that a thin film standard of known thickness, known composition and density must be manufactured for each element of interest. The problem introduced by this method is the thickness determination, which can be only done in a sufficiently accurate way by means of convergent beam electron diffraction (CBED). Since thickness measurements by CBED can be a time consuming procedure which is also restricted to thick, crystalline specimens, only a few examples of the application of the standard method have been published.

One example of the application of this method was published by Crozier [19], who measured absolute cross-sections for the elements C, Al, Fe, Cu and Ag. Crozier used thin evaporated films thicknesses of which were measured by weighing.

The problems of such measurements lie in the fact that in very thin metal films thin oxide layers due to air oxidation, and contamination films may introduce considerable systematic errors in the determination of cross-sections. If thicker samples are used the effect of thin oxidation layers decreases but the spectrum has to be corrected for multiple scattering.

3.2.2 *k-factor method.* — The above mentioned difficulties can be partially avoided if ratios of cross-sections are determined [20,21].

Efficient quantification can be obtained using compound standards. In this method, a thin film standard is used which must contain one standard light element (B) which gives a K-edge in the EELS-spectrum and the element (A) the cross-section of which is sought.

If the concentration of these two elements is known, the cross-section ratio can be determined

according to the following equation:

$$\frac{\sigma_B(\beta,\Delta)}{\sigma_A(\beta,\Delta)} = \frac{I_B(\beta,\Delta)}{I_A(\beta,\Delta)} \cdot \frac{N_A}{N_B} = k_{AB}$$

The measured cross-section ratios can be viewed as EELS-k-factors in analogy to thin film EDX. Absolute cross-section values can be determined by using a calculated cross-section value for the light element. This can be done, because the K-edges of light elements can be accurately calculated.

Preferably, oxide compounds should be used for k-factor determinations, although boride compounds can also be used successfully as shown by Malis and Titchmarsh [20]. From our point of view oxide compounds [21] provide some essential advantages: An accurate intensity of the K-edge of oxygen in the medium energy-loss region (at 532 eV) is relatively easy to measure, because there are no background extrapolation problems as associated with low energy edges and no problems with low count rates as with higher energy losses. Finally, oxides can be easily prepared and frequently have stoichiometric compositions.

At the present state of development the k-factor approach has some essential advantages:

1) All elements and all energy-loss(edges (K, L, M, N and O-edges) can be quantified with good accuracy.
2) Thickness determination is not necessary.
3) Contamination layers or thin amorphous layers do not disturb the measurement of intensity ratios.
4) Cross-section ratios show a smaller dependence on multiple scattering, because its effect on each edge cancels [22].
5) k-factors can be viewed as effective "cross-sections" to take account of lens abberation effects.

Furthermore, it turns out that cross-section ratios are not as dependent on the experimental conditions as absolute cross-sections. Therefore, published k-factors make possible efficient EELS-quantification of data obtained under fairly similar experimental conditions in other laboratories.

4. Comparison of experimental and theoretical cross-sections.

4.1 K-EDGES. — Energy-loss spectroscopy is useful because it can detect elements lighter than Na from their K-shells. K-edges generally show a simple saw-tooth profile that can be easily described by hydrogenic wavefunctions and by Hartree-Slater-wavefunctions.

We first of all investigate the degree to which the alternative theoretical models differ in their prediction of cross-section for K-edges (Tab. I). The C K, N K and O K edges have been calculated with the Hydrogenic and Hartree-Slater model for an incident electron energy of 120 kV, a collection angle of 5.9 mrad and a large energy window (Δ = 100 eV). The values obtained with these two methods differ typically by 10% which is already more than the typical experimental error involved in EELS-measurements. This is in contradiction to results of Egerton [11] and Rez [14], who found a good agreement (< 5%) between Hartree-Slater values and hydrogenic values which have been calculated with the SIGMAK1 program. However, an improved version of the hydrogenic model (SIGMAK2) incorporates retardation and exact relativistic kinematics [3] which increases partial cross-sections by typically 10% thus giving larger differences to Hartree-Slater values.

In figure 1, hydrogenic cross-sections are compared with experimental values which have been determined from k-factors [4,20]. Crozier's values [19] obtained by absolute measurements are

Table I. — *Comparison of calculated cross-sections for K-edges* $[cm^2/atom]$ *for* E_0 *=120 kV,* β *=5.9 mrad and* Δ *=100 eV.*

Edge	Hartree-Slater	Hydrogenic	Difference
C K	4.145×10^{-21}	4.811×10^{-21}	13.8%
N K	1.909×10^{-21}	2.097×10^{-21}	10.0%
O K	9.327×10^{-22}	1.037×10^{-21}	9.0%

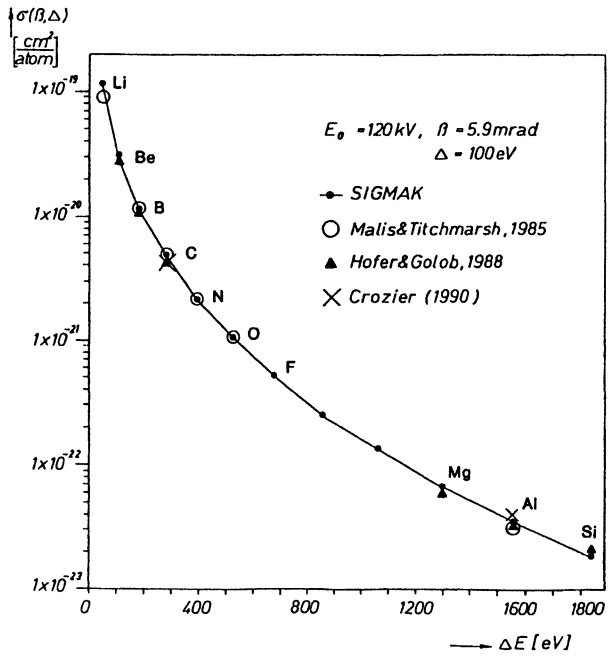

Fig. 1. — K-edges: Comparison of experimental partial cross-sections with cross-sections calculated by the hydrogenic model (SIGMAK) for $E_0 = 120$ keV, $\beta = 5.9$ mrad and $\Delta = 100$ eV.

also included. All measured values lie within 10% of the hydrogenic model thus demonstrating that the use of the calculated cross-sections for the quantification of light elements is reasonable (see also [23]).

This is only true when larger energy windows ($\Delta > 50$ eV) are used. In this case near-edge fine structures will be averaged out and the differences between calculated and experimental integrated intensity will be less than 10% [4,24]. However, in case of smaller energy windows ($\Delta < 50$ eV) near-edge fine structures can have more influence on edge intensities, and calculated cross-sections should be used with caution. Therefore, quantification should be performed by means of experimental k-factors. This statement can be extended to all other edges like L, M and N edges as well.

4.2 L_{23}-EDGES. — The elements Mg-As give rise to L_{23}-ionizations in the energy-region accessible by EELS (0-2000 eV) and can be analyzed using these L_{23}-edges.

A difficulty associated with the L-edges lies in the fact that the edge profile is not as simple as in the case of the K-edges. The elements Mg-Ar and the elements Zn-As exhibit an edge with a delayed maximum and the elements K to Cu further give rise to narrow and intense peaks at the edge onset (white lines). As already mentioned, partial cross-sections for the elements Al to Zn can be calculated with the hydrogenic model and the Hartree-Slater model allows the calculation of L-edges for the elements Mg to As.

Figure 2 shows the cross-section ratios (k-factors) for the elements ranging from Al to Ge for the above mentioned experimental conditions. Besides our results [4] values measured by Malis and Titchmarsh [20], Crozier [19] and Grande and Ahn [25] are included.

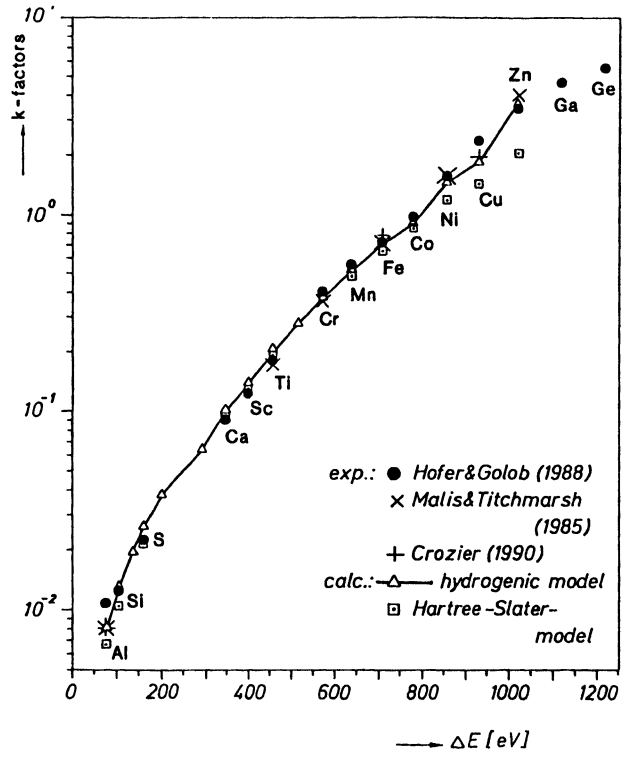

Fig. 2. — L_{23}-edges: Comparison of experimental k-factors with k-factors calculated using the hydrogenic model (SIGMAL2) and the Hartree-Slater model for $E_0 = 120$ keV, $\beta = 5.9$ mrad and $\Delta = 100$ eV.

While in case of the elements Ca to Co the agreement between hydrogenic, Hartree-Slater and experimental k-factors is quite good (within 10%), there are severe differences for the elements Al to S and Ni to Zn (up to 50%).

In Al and Si L-edges problems arise with the background fitting, because the near plasmon peak can give rise to a background of complex shape. Additionally problems with multiple scattering processes can be significant.

In case of Ni, Cu and Zn the experimental and hydrogenic values show good agreement (within

10%), but the Hartree-Slater values for these elements deviate by as much as 50%. Calculated k-factors for Ga and Ge are not available.

One explanation for this result is that the SIGMAL2-program has been fitted to experimentally determined data and therefore white lines are included to some extend [3]. At this point, it must again be emphasized that the Hartree-Slater-theory only deals with transitions to unoccupied continuum states and does not take into account transitions towards bound states involved in the white lines.

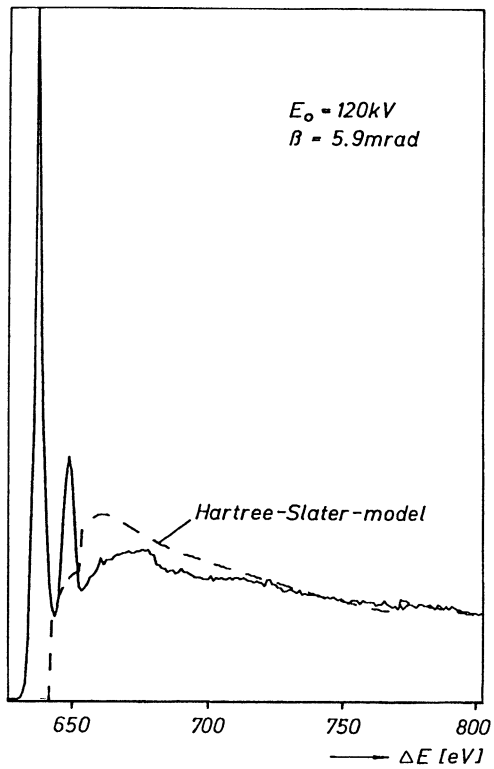

Fig. 3. — Spectrum of the Mn L_{23} edge from MnO (solid line) compared with the Hartree-Slater calculation (dashed line) (from [24]).

This is demonstrated in figure 3, where the experimental L_{23}-edge of manganese is compared with the Hartree-Slater edge profile. The calculated profile is scaled to experiment by normalizing to the experimental data 100eV beyond threshold where the intensity could be attributed solely to continuum transitions. A direct and fair comparison of Hartree-Slater-theory and experimental data is therefore only possible after removal of the white line portion in the spectra. This has been done recently by Auerhammer *et al.* (26). A comparison of Auerhammer's values (white line extracted) with our data (white lines included) shows that the k-factors obtained by the Hartree-Slater theory exhibit a better agreement with our data than with Auerhammer's (see Tab. II).

Since the white lines are a very useful signal for microanalysis and since we try to use all available data and not only part of them, we did not remove the white lines from our spectra.

Another interesting aspect is how quantification results depend on the integration regions Δ.

Table II. — *k-factors for some L_{23}- and M_{45}-edges with white lines at the threshold (E_0 =120 keV, Δ =100 eV, β =5.9 mrad).*

Edge	experimental		calculated	
	with w.l. [4]	without w.l. [26]	H.S. [26]	Hy.
Mn L_{23}	0.549	0.725	0.485	0.518
Fe L_{23}	0.704	0.870	0.654	0.690
Co L_{23}	0.962	1.24	0.862	0.893
Ni L_{23}	1.57	2.02	1.17	1.45
Ba M_{45}	0.351	0.535	0.333	
Pr M_{45}	0.539	1.14	0.671	
Dy M_{45}	2.16	4.24	2.44	

This is demonstrated for the two versions of the hydrogenic model SIGMAL1 and the newer SIGMAL2. Figure 4, showing the quantification of Fe_2O_3 for various energy-windows and collection angles, illustrates that SIGMAL2 provides more stable results. If SIGMAL2 is used for quantification good results for small energy-windows such as 25eV can be obtained. SIGMAL2 takes almost full account of the experimental edge shapes. Similar results have been reported recently by Manoubi *et al.* [27].

To summarize, it appears that the hydrogenic model cross-sections provide a rather satisfactory agreement with experimental data and are very useful for microanalytical applications. For the quantification of elements heavier than zinc Hartree-Slater values or experimental *k*-factors have to be used.

4.3 M_{45}-EDGES. — At the present state of instrumental EELS-development the elements from Sr to W can only be analyzed by the M_{45}-edges. The corresponding M-cross-sections can be calculated by means of the Hartree-Slater model [14] and by a hydrogenic approach [13] as well.

The M_{45}-edges of the lanthanides and of Cs and Ba exhibit a good peak to background ratio due to the white lines. Therefore these white lines are not omitted from the experimental data.

In figure 5 *k*-factors for the elements Sr to W are presented. The Hartree-Slater-values are compared with our experimental *k*-factors [29,30] for the above mentioned experimental conditions. In case of the elements ranging from Sr to Cd the theory gives ratios that can be as much as 50% different from the experimental results. Since the M_{45}-edges of the elements Sr to Cd have no white line at the edge threshold, the disagreement between theory and experiment can only be caused by the broad delayed edges of these elements. However, there is satisfactory agreement ($< 10\%$) in case of Ta and W which give rise to delayed edges as well.

Varying results have been found for the rare earth elements: While the calculated *k*-factors for Ba, Nd, Eu, Dy, Ho and Er are within 15% of the experimental values the other rare earth elements exhibit severe differences. For comparison, the results of Crozier [19] and Chadwick and Malis [27] scaled from their experimental conditions to ours [29,30] have been included in the diagram (Fig. 5) and are consistent with the trend revealed by our experiments.

Recently, Manoubi *et al.* [31] published an experimental determination of *k*-factors of the rare earth elements. For a clearer visibility of the various results we compare the experimental and theoretical results in a separate diagram: In figure 6 the Hartree-Slater values are compared with the experimental *k*-factors (including the white lines).

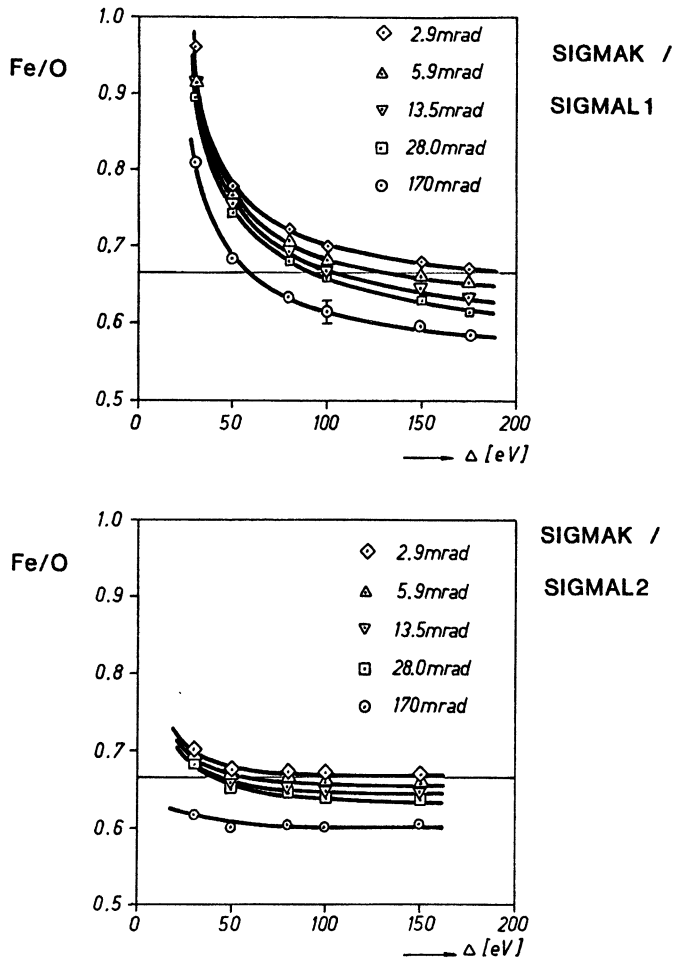

Fig. 4. — Quantification of spectra of Fe_2O_3 with (a) the SIGMAL1 and (b) the SIGMAL2 program for E_0 = 120keV. The dependence of the Fe/O atomic ratio upon energy window is shown for collection angles ranging from 2.9 to 170 mard (from [4]).

From Ce to Ho, there is very good agreement between the experiments, but the Hartree-Slater values are significantly higher. For the elements La, and Er to Lu Manoubi's values agree better with the Hartree-Slater theory than with our values. As the Hartree-Slater model ignores the white lines which are very prominent in the case of the lanthanides (30-40% of the total intensity of the M_{45}-edge at Δ = 100 eV) and the white lines are included in the experimental values, it is not surprising, that there is a significant difference between theory and experiment. If the white lines are subtracted from the measured M-edges the agreement between theory and experiment becomes worse as shown in table II. Concerning the differences between the experimental values for the elements Er to Lu one must take into account that the data have been recorded under different experimental conditions (image coupling [31] vs. diffraction coupling [29,30]).

Summarizing, one can state that at the present state of development, quantification of M-edges should be performed with experimental k-factors. This is especially necessary if smaller energy windows are used for determination of edge intensities.

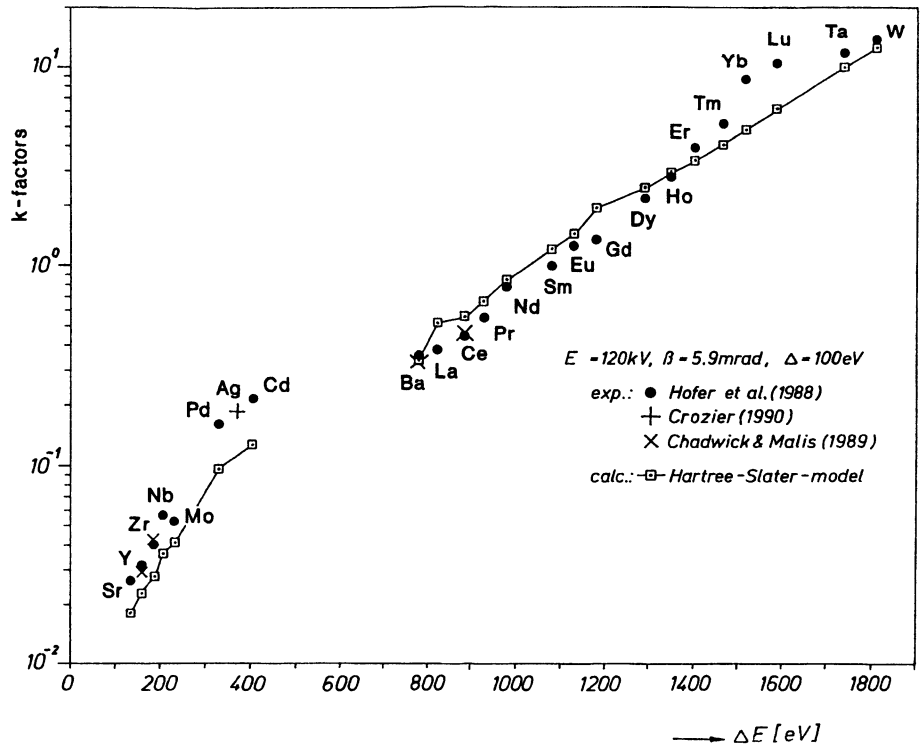

Fig. 5. — M_{45}-edges: Comparison of experimental k-factors with k-factors calculated using the Hartree-Slater model for the elements Sr to W for E_0 = 120keV, β = 5.9mrad and Δ = 100eV.

4.4 N_{45}-EDGES. — Cs, Ba and the rare earth elements have two groups of transitions within the range of most EELS-spectrometers. Besides the sharp well-defined M_{45}-edges, intense N_{45}-transitions arise in case of these elements in the energy-loss region from 80 eV to 200 eV. These N_{45}-absorption edges are due to transitions of 4d electrons into unoccupied states of the partially filled 4f shell. These N-edges cannot be predicted by an atomic or single electron model [15]. Therefore, the scattering cross-sections of the N_{45}-edges are only accessible by experimental work.

The N_{45}-edges of the lanthanides and of Cs and Ba exhibit a very intense signal with a good peak to background ratio and therefore these edges may be useful for microanalysis.

We measured the k-factors for the elements Ba to Tm by means of the corresponding oxides in the form of thin films [32]. Figure 7 includes values for three different energy windows: 30, 50 and 100 eV. The data exhibit the change of the edge shapes of the N_{45}-edges, i.e. in case of the elements Ba to Nd most intensity lies within the first 50eV above the edge onset, while the N_{45}-intensity of the higher rare earth elements is distributed over larger energy-loss regions.

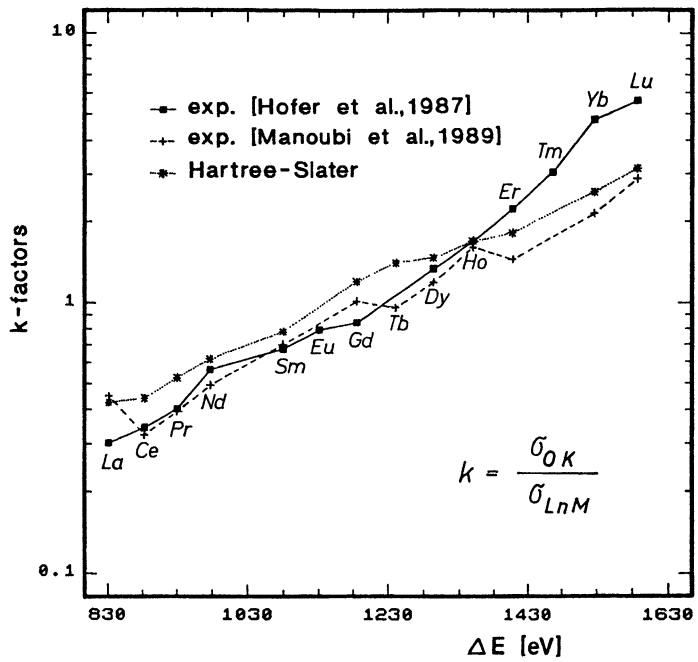

Fig. 6. — M_{45}-edges: k-factors for the lanthanides ($E_0 = 120$ keV, $\beta = 22$ mrad and $\Delta = 100$ eV).

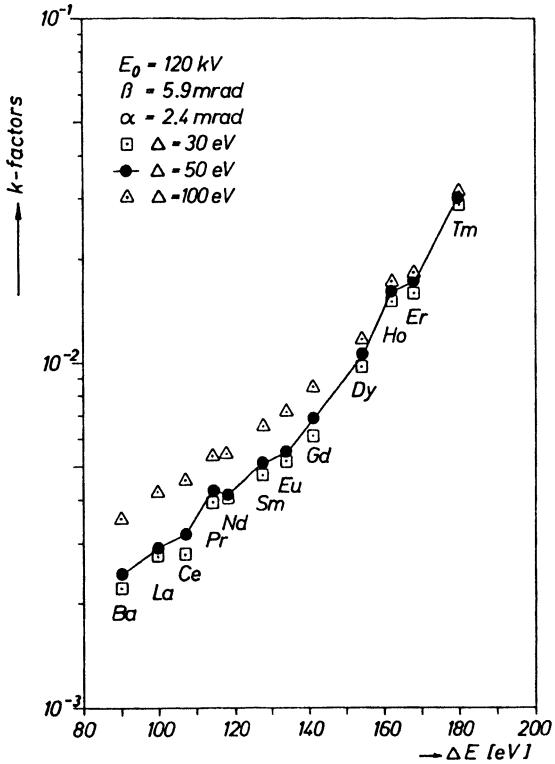

Fig. 7. — N_{45}-edges: k-factors for the lanthanides ($E_0 = 120$ keV, $\beta = 5.9$ mrad).

5. Practical quantification examples.

In this section we apply the k-factor approach to the quantification of EELS-spectra of chemical compounds consisting of light and heavier elements. The results are shown in table III:

Table III. — *Quantification results for EELS-spectra of compounds consisting of both light and heavy elements. The spectra have been quantified by using experimentally determined k-factors. The experimental conditions are: E_0 =120 keV, β =5.9 mrad and Δ =50 eV.*

$Nd_2Ti_2O_7$ with Nd M_{45}, TiL_{23} and O K edge

	expected [at%]	found [at%]
Nd	18.2	17.0 ± 0.9
Ti	18.2	19.1 ± 0.5
O	63.6	63.9 ± 1.2

$BaTiO_3$ with Ba M_{45}, TiL_{23} and O K edge

	expected [at%]	found [at%]
Ba	20.0	18.4 ± 0.3
Ti	20.0	20.5 ± 0.5
O	60.0	61.1 ± 0.6

LaB_6 with La N_{45}, B K and O K edge

	expected [at%]	found [at%]
La	14.3	15.9 ± 0.4
B	85.7	78.8 ± 1.3
O	–	5.3 ± 0.2

PrB_6 with Pr N_{45}, B K and O K edge

	expected [at%]	found [at%]
Pr	14.3	16.1 ± 0.5
B	85.7	81.0 ± 1.5
O	–	2.9 ± 0.2

$Nd_2Ti_2O_7$ and $BaTiO_3$ have been chosen to demonstrate the quantification of K, L and M-edges. In both cases, the measured concentrations are fairly close to those expected from the chemical formulae.

To demonstrate the use of the N_{45}-edges rare earth borides have been analyzed: The spectra have been quantified using the N-edge of the rare earth element and the K-edge of boron (and oxygen). Again the measured values are fairly close to those expected from the chemical formulae. However, it is not clear if the oxygen found is an impurity in the sample or if it is caused by a thin oxidation layer.

6. Conclusions.

The comparison of theoretical and experimental data for core-loss transitions shows that in case of K and L edges good agreement exists (for larger energy windows) and in case of M and N edges severe differences can occur. To determine the origin of the observed spread in case of some experimental data, further experiments seem desirable. To reduce background extrapolation errors, small energy windows should be used for the determination of edge intensities. However, calculated cross-sections for small energy windows ($\Delta < 50$ eV) are uncertain due to the near edge fine structures and white lines. Therefore experimental k-factors should be used for smaller energy windows. If experimental k-factors are used for the quantification of light elements, an accuracy of about 5 rel% seems attainable. In case of heavier elements ($Z > 30$) one can expect 5 to 10 rel%.

Recently, improvements in background subtraction [33-36] and modelling of overlapping edges [27,37,38] have been suggested and these methods will further improve the accuracy of EELS-quantification in the near future. Finally, as discussed elsewhere at this workshop, the increasing application of parallel EELS-detection systems will greatly reduce spectrum collection times and certain accompanying collection errors. In conclusion, then, it can be expected that EELS may soon be as accurate as EDX-microanalysis of thin films.

Acknowledgements.

I am grateful to Dr. Peter Rez (Arizona State University, USA) for the calculation of Hartree-Slater cross-sections, to Dr. B. Luo (Fritz Haber Institut Berlin, Germany) for providing new EELS quantification software and to Dr. T.F. Malis (CANMET Ottawa, Canada) for a compilation of EELS-k-factors.

Appendix.

Experimental k-factors and dipole oscillator strengths for K, L_{23}, M_{45} and N_{45} ionizations:

The experimental k-factors have been determined for $E = 120$ keV, $\beta = 5.9$mrad, $\Delta = 50$ and 100 eV and have been taken from references 4, 28, 29 and 31 (revisements in case of Be K, Al L_{23}, Si L_{23} and Sr M_{45} edges).

The dipole oscillator strengths have been calculated from the k-factors using a program written by R.F. Egerton [1]. $f(50)$ and $f(100)$ for oxygen have been taken as 0.22 and 0.41 (calculated from Hartree-Slater values).

K-edges:

	$\Delta = 50$ eV			$\Delta = 100$ eV		
	σ_{OK}/σ_{XK}	*%	$f(50)$	σ_{OK}/σ_{XK}	*%	$f(100)$
Be	0.0305	4.9	0.696	0.0382	5.4	1.21
B	0.0820	2.5	0.511	0.0971	2.5	0.861
C	0.226	2.7	0.337	0.256	3.8	0.576
N				0.488	6.4	0.511
O	1.000		0.22	1.000		0.41
Mg	17.5	7.5	0.0847	16.20	6.8	0.165
Al	34.0	4.1	0.0683	30.77	5.3	0.135
Si	49.5	7.9	0.0722	46.7	5.9	0.136

L_{23}-edges:

	Δ = 50 eV			Δ = 100 eV		
	σ_{OK}/σ_L	[%]*	$f(50)$	σ_{OK}/σ_L	[%]*	$f(100)$
Al	0.010	2.1	1.30	0.0108	2.5	2.63
Si	0.0126	1.4	1.49	0.0126	1.6	3.11
S	0.0236	5.5	1.49	0.0223	7.9	3.18
Ca	0.0820	2.7	1.27	0.0840	4.5	2.37
Sc	0.113	3.8	1.18	0.1242	4.1	2.03
Ti	0.162	2.9	1.01			
Cr	0.358	2.3	0.702	0.392	2.6	1.19
Mn	0.538	2.4	0.575	0.549	2.5	1.04
Fe	0.676	1.9	0.559	0.704	2.1	0.987
Co	1.01	1.5	0.456	0.962	1.4	0.836
Ni	1.87	1.4	0.299	1.57	1.7	0.649
Cu	3.16	2.3	0.213	2.35	1.6	0.522
Zn	4.93	3.3	0.168	3.42	3.3	0.439
Ga	7.04	3.7	0.144	4.65	3.2	0.396
Ge	14.6	6.4	0.086	5.59	4.7	0.404

M_{45}-edges:

	Δ = 50 eV			Δ = 100 eV		
	σ_{OK}/σ_M	[%]*	$f(50)$	σ_{OK}/σ_M	[%]*	$f(100)$
Sr	0.0439	11.3	0.611	0.0266	6.8	2.07
Y	0.0543	5.4	0.621	0.0317	4.3	2.15
Zr	0.0712	2.9	0.559	0.0400	2.5	1.99
Nb	0.120	3.7	0.399	0.0558	1.1	1.70
Mo	0.103	5.9	0.534	0.0522	5.9	2.07
Pd	0.438	4.9	0.225	0.159	3.8	1.19
Cd	0.498	6.5	0.270	0.211	6.8	1.20
Ba	0.331	3.8	1.40	0.351	3.2	2.41
La	0.331	3.9	1.59	0.376	4.0	2.57
Ce	0.370	4.4	1.62	0.441	2.2	2.49
Pr	0.481	1.2	1.40	0.539	1.6	2.28
Nd	0.693	1.7	1.08	0.768	3.6	1.78
Sm	0.883	2.6	1.07	0.979	2.1	1.75
Eu	1.11	1.1	0.947	1.22	1.3	1.56
Gd	1.24	3.7	0.948	1.30	3.1	1.63
Dy	2.04	3.8	0.713	2.16	3.5	1.21
Ho	2.79	4.3	0.578	2.81	3.3	1.03
Er	3.98	3.0	0.450	3.86	2.2	0.835
Tm	5.90	5.1	0.336	5.12	4.9	0.696
Yb	11.3	5.1	0.195	8.68	5.9	0.453
Lu	19.1	9.5	0.128	10.3	9.5	0.423
Ta	18.6	2.2	0.165	11.9	2.1	0.459
W	19.7	7.6	0.174	13.8	4.4	0.443

N_{45}-edges:

	$\Delta = 50$ eV			$\Delta = 100$ eV		
	σ_{OK}/σ_N	[%]*	$f(50)$	σ_{OK}/σ_N	[%]*	$f(100)$
Ba	2.42×10^{-3}	3.5	7.11	4.06×10^{-3}	3.6	9.03
La	2.88×10^{-3}	4.3	6.43	4.14×10^{-3}	4.7	9.46
Ce	3.18×10^{-3}	2.4	6.60	4.56×10^{-3}	2.8	9.65
Pr	4.27×10^{-3}	3.1	5.13	5.31×10^{-3}	4.1	8.62
Nd	4.14×10^{-3}	1.9	5.52	5.37×10^{-3}	1.9	8.86
Sm	5.15×10^{-3}	2.4	5.01	6.46×10^{-3}	3.0	8.24
Eu	5.47×10^{-3}	3.6	4.90	6.65×10^{-3}	3.6	8.29
Gd	6.93×10^{-3}	4.2	4.13	8.47×10^{-3}	4.0	6.91
Dy	1.07×10^{-2}	1.4	3.00	1.21×10^{-2}	4.1	5.39
Ho	1.65×10^{-2}	4.2	2.06	1.68×10^{-2}	8.0	4.09
Er	1.71×10^{-2}	4.2	2.11	1.81×10^{-2}	4.4	4.00
Tm	3.01×10^{-2}	3.8	1.28	3.08×10^{-2}	4.5	2.51

References

[1] EGERTON R.F., these proceedings.
[2] EGERTON R.F., *Ultramicroscopy* **3** (1978) 243.
[3] EGERTON R.F., Electron Energy-Loss Spectroscopy in the Electron Microscope (Plenum Press), 1986.
[4] HOFER F. and GOLOB P., *Micron Microscopica Acta* **19** (1988) 73.
[5] SWYT C.R. and LEAPMAN R.D., Scanning Electron Microscopy, O. Johari Ed. (Chicago - AMF O'Hare 1982), vol. I, 73.
[6] EGERTON R.F., WILLIAMS B.G. and SPARROW T.G., *Proc. Roy. Soc. Lond.* **A398** (1985) 395.
[7] CRAVEN A.J., BUGGY T.W. and FERRIER R.P., in: Quantitative Microanalysis with High Spatial Resolution, (The Metals Society, London, 1981) p. 141.
[8] ZALUZEC N.J., HREN J.J. and CARPENTER R.W., Proc. 38th Ann. EMSA Meeting, G.W. Bailey Ed. (Claitor's Publishing Baton Rouge, Louisiana, 1980) p. 114.
[9] TITCHMARSH J.M. and MALIS T.F., *Ultramicroscopy* **28** (1989) 277.
[10] EGERTON R.F., *Ultramicroscopy* **4** (1979) 169.
[11] EGERTON R.F., Scanning Electron Microscopy, O. Johari Ed. (Chicago - AMF O'Hare 1984), vol. II, 505.
[12] EGERTON R.F., Proc.39th Ann. EMSA Meeting, G.W. Bailey Ed. (Claitor's Publishing Baton Rouge, Louisiana, 1981) p. 198.
[13] LUO B. and ZEITLER E., submitted to *J. Chem. Phys.*
[14] LEAPMAN R.D., REZ P. and MAYERS D.F., *J. Chem. Phys.* **72** (1980) 1232.
REZ P., *Ultramicroscopy* **9** (1982) 283.
[15] AHN C.C. and REZ P., *Ultramicroscopy* **17** (1985) 105.
REZ P., *Ultramicroscopy* **28** (1989) 16.
[16] SKIFF W.M., CARPENTER R.W., LIU S.H. and HIGGS A., *Ultramicroscopy* **25** (1988) 47.
[17] SCHORSCH P., WEICKENMEIER A. and KOHL H. (in preparation).
[18] JOY D.C., EGERTON R.F. and MAHER D.M., Scanning Electron Microscopy, O. Johari Ed. (Chicago - AMF O'Hare 1979) Vol. II, p. 817.
[19] CROZIER P.A. and EGERTON R.F., EMAG'87 Analytical Electron Microscopy, G.W. Lorimer Ed. (London, Institute of Metals, 1988) p. 103.
CROZIER P.A., *Philos. Mag. B* **61** (1990) 311.
[20] MALIS T.F. and TIRCHMARSH J.M., *Inst. Phys. Conf. Ser.* **78** (1985) 181.

MALIS T.F., RAJAN K., TITCHMARSH J.M. and WEATHERLY G.C., Intermediate Voltage Microscopy and Its Application to Materials Science (Philips, Mahway, NJ, 1986) p. 78.
[21] HOFER F., *Ultramicrosc.* **21** (1987) 63.
[22] BOURDILLON A.J. and STOBBS W.M., *Ultramicrosc.* **17** (1985) 147.
[23] BRYDSON R.D., WILLIAMS B.G., ENGEL W., LINDNER T., MUHLER M., SCHLÖGL R., ZEITLER E. and THOMAS J.M., *J. Chem. Soc., Faraday Trans. 1* **84** (1988) 631.
[24] WENG X. and REZ P., *Ultramicroscopy* **25** (1988) 345.
[25] GRANDE M. and AHN C.C., *Inst. Phys. Conf. Ser.* **10** (1983) 123.
[26] AUERHAMMER J., REZ P. and HOFER F., *Ultramicroscopy* **30** (1989) 365.
[27] MANOUBI T., TENCE M., WALLS M.G. and COLLIEX C., *Microsc. Microanal. Microstruct.* **1** (1990) 23.
[28] CHADWICK M.M. and MALIS T.F., *Ultramicroscopy* **31** (1989) 205.
[29] HOFER F., GOLOB P. and BRUNEGGER A., EMAG'87 Analytical Electron Microscopy, G.W. Lorimer Ed. (The Institute of Metals, London, 1988) p. 119.
[30] HOFER F., GOLOB P. and BRUNEGGER A., *Ultramicroscopy* **25** (1988) 81.
[31] MANOUBI T., REZ P. and COLLIEX C., *J. Elect. Spect. Relat. Phenom.* **50** (1990) 1.
[32] HOFER F., *J. Microsc.* **156** (1989) 279.
[33] STEELE J.D., TITCHMARSH J.M., CHAPMAN J.N. and PATERSON J.H., *Ultramicroscopy* **17** (1985) 273.
[34] TREBBIA P., *Ultramicroscopy* **24** (1988) 266.
[35] LIU D.R. and WILLIAMS D.B., Proc. 45th Ann. EMSA Meeting, G.W. Bailey Ed. (Claitor's Publishing Baton Rouge, Louisiana, 1987) p. 118.
[36] LIU D.R. and BROWN L.M., *J. Microsc.* **147** (1987) 37.
[37] BAUER H.D. and SCHOLZ W., *Ultramicroscopy* **23** (1987) 109.
[38] LEAPMAN R.D. and SWYT C.R., *Ultramicroscopy* **26** (1988) 393.